

THE WARPED NUCLEAR DISK OF RADIO GALAXY 3C 449

GRANT R. TREMBLAY¹, ALICE C. QUILLEN¹, DAVID J. E. FLOYD², JACOB NOEL-STORR³, STEFI A. BAUM⁴, DAVID AXON⁵,
 CHRISTOPHER P. O'DEA⁵, MARCO CHIABERGE^{2,6}, F. DUCCIO MACCHETTO², WILLIAM B. SPARKS², GEORGE K. MILEY⁷,
 ALESSANDRO CAPETTI⁸, JUAN P. MADRID², AND ERIC PERLMAN⁹

Accepted for publication in ApJ, 1/24/06

ABSTRACT

Among radio galaxies containing nuclear dust disks, the bipolar jet axis is generally observed to be perpendicular to the disk major axis. The FR I radio source 3C 449 is an outlier to this statistical majority, as it possesses a nearly parallel jet/disk orientation on the sky. We examine the 600 pc dusty disk in this galaxy with images from the *Hubble Space Telescope*. We find that a $1.6\ \mu\text{m}/0.7\ \mu\text{m}$ colormap of the disk exhibits a twist in its isocolor contours (isochromes). We model the colormap by integrating galactic starlight through an absorptive disk, and find that the anomalous twist in the isochromes can be reproduced in the model with a vertically thin, warped disk. The model predicts that the disk is nearly perpendicular to the jet axis within 100 pc of the nucleus. We discuss physical mechanisms capable of causing such a warp. We show that precessional models or a torque on the disk arising from a possible binary black hole in the AGN causes precession on a timescale that is too long to account for the predicted disk morphology. However, we estimate that the pressure in the X-ray emitting interstellar medium is large enough to perturb the disk, and argue that jet-driven anisotropy in the excited ISM may be the cause of the warp. In this way, the warped disk in 3C 449 may be a new manifestation of feedback from an active galactic nucleus.

Subject headings: galaxies: active — galaxies: individual (3C 449) — galaxies: ISM

1. INTRODUCTION

Imaging campaigns have established that radio-loud elliptical galaxies can host gaseous disks in their central few hundred parsecs, thought to be feeding the massive $10^9 M_\odot$ black holes at their centers (e.g., Ferrarese et al. 1996; Jaffe et al. 1996; Ferrarese & Ford 1999). Visible and radio images of normal and radio-loud elliptical galaxies can be used to probe the relation between the orientation of the jets and the morphology of the gas and dust near the nucleus. Ground based studies first discovered a connection, finding that dusty disks are often nearly perpendicular to radio jets (Möllenhoff, Hummell, & Bender 1992; Kotanyi & Ekers 1979). These studies supported the widely held expectation that there is a link between the angular momentum of accreting material and the orientation of the jet axis. Subsequent surveys of the observed angular difference on the sky, Ψ_{JD} , between bipolar jet and disk major axes in radio galaxies found a statisti-

cally significant peak in the distribution at $\Psi_{JD} \approx 90^\circ$ (Möllenhoff, Hummell, & Bender 1992; Kotanyi & Ekers 1979; Martel et al. 2000; van Dokkum & Franx 1995; de Koff et al. 2000; Verdoes Kleijn et al. 1999). Taking 3D jet orientation into account and correcting for beaming effects, Sparks et al. (2000) also showed that these disks are generally orthogonal to jet axes. The correlation could be stronger for FR I type sources than FR II types (de Koff et al. 2000; Fanaroff & Riley 1974), and as of yet, no strong trend between the jet axis and the galactic isophotal major axis is known to exist in low redshift objects (e.g., Sansom et al. 1987; Kinney et al. 2000).

More recent examinations of 3D jet/disk orientations have found additional complexities in the distribution. The statistical work by Verdoes Kleijn & de Zeeuw (2005) found that dust *lanes* are nearly perpendicular to jets, whereas dusty disks with ellipsoidal edges have a wide range of intrinsic jet/disk orientation angles. Schmitt et al. (2002) showed that projection effects of radio and gaseous structures on the sky must be taken into account in any such study of jet/disk orientations. This work demonstrated that the statistical distribution of Ψ_{JD} is consistent with a homogeneous three dimensional angular distribution that is modified by including a cone of avoidance. The cone corresponds to an absence of jet axes lying within $\sim 13 - 25^\circ$ of the plane of the disk. This may suggest that jet/disk orthogonality is not a trend, but simply a manifestation of the cone of avoidance in the underlying distribution of relative orientations (Schmitt et al. 2002). The notion that disks are intrinsically perpendicular to jets (Verdoes Kleijn & de Zeeuw 2005) may also be an artifact of observational biases and small sample sizes, or because only a restricted class of objects exhibit jet/disk orthogonality.

¹ Department of Physics and Astronomy, University of Rochester, Rochester, NY 14627; grant@pas.rochester.edu; aquillen@pas.rochester.edu

² Space Telescope Science Institute, 3700 San Martin Dr., Baltimore, MD 21218; floyd@stsci.edu

³ Steward Observatory, University of Arizona, Tucson, AZ 85721

⁴ Center for Imaging Science, Rochester Institute of Technology, 54 Lomb Memorial Drive, Rochester, NY 14627

⁵ Department of Physics, Rochester Institute of Technology, 54 Lomb Memorial Drive, Rochester, NY 14627

⁶ On leave from INAF—Istituto di Radioastronomia, Via P. Gobetti 101, Bologna I-40129, Italy

⁷ Leiden Observatory, P.O. Box 9513, NL-2300 RA Leiden, The Netherlands

⁸ INAF—Osservatorio Astronomico di Torino, Strada Osservatorio 20, 10025 Pino Torinese, Italy

⁹ Joint Center for Astrophysics, Department of Physics, University of Maryland, Baltimore County, 1000 Hilltop Circle, Baltimore, MD 21250

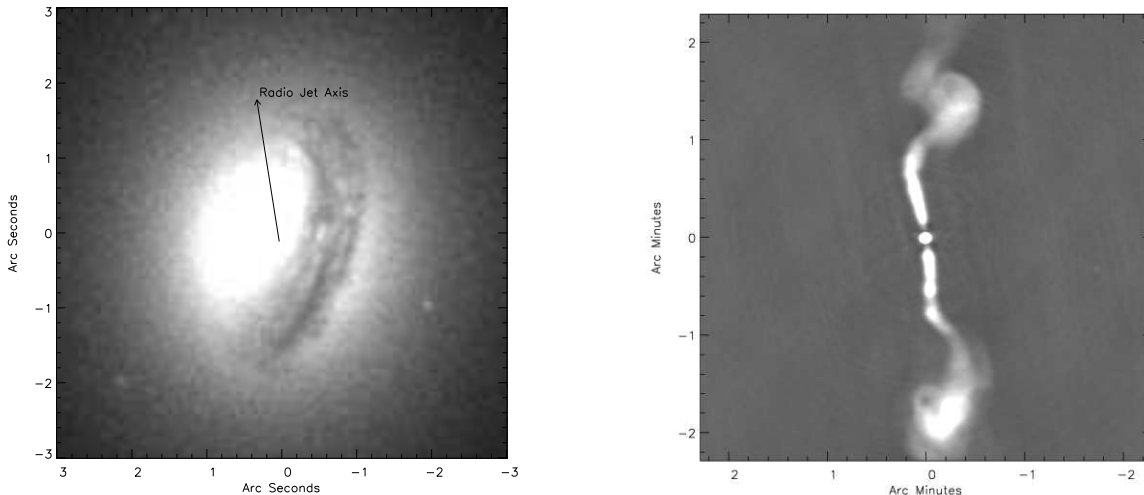


FIG. 1.— a) *HST*/ *WFPC2* $0.7\ \mu\text{m}$ image of 3C 449. Here the highly inclined nuclear disk is clearly visible. b) 4.8 GHz *VLA* image of the radio structure of 3C 449. At a distance of 73 Mpc, one arcminute corresponds to ~ 21 kpc.

An additional complication in the interpretation of any Ψ_{JD} distribution arises from the sometimes disturbed morphology of gaseous structures in the heart of many radio galaxies (e.g., Martel et al. 2000; de Koff et al. 2000; van Dokkum & Franx 1995). Such studies suggest that many of these disks are not dynamically stable or relaxed in the galactic potential. Detailed observations of gaseous structure in individual galaxies have also found evidence for non-planar or warped geometries (e.g., de Koff et al. 2000; van Dokkum & Franx 1995, Ferrarese & Ford 1999 in NGC 6251 and Quillen & Bower 1999 in M84). Furthermore, Noel-Storr et al. (2005) presents an emission-line study of gas kinematics in the heart of radio galaxies, finding that many such structures are not consistent with a thin Keplerian disk model.

In a non-spherical quiescent galaxy, dust and gas settle into a galactic symmetry plane on timescales of order 10-100 times the rotation period at a given radius (Steiman-Cameron & Durisen 1988). Previous studies have shown that the dust in elliptical galaxies is likely external in origin, and settles into the galactic equatorial plane after several dynamical timescales following a merger (e.g., Tran et al. 2001; de Koff et al. 2000; Goudfrooij & de Jong 1995; Lauer et al. 2005). Gas that does not reside in the principle symmetry plane of a galaxy must have been injected or perturbed on a timescale shorter than this. Since the rotation period is short near the nucleus (approximately 2 million years at 100 pc in a luminous elliptical galaxy), we would expect to find the majority of nuclear gas disks residing in a symmetry plane of their host galaxies. As such, we would not expect a link between the orientations of $\sim 10^2$ pc sized gas disks and radio jets. Instead, we generally expect to find settled, planar, and quiescent nuclear disks in the symmetry plane of the galaxy. Nevertheless, disturbed dust morphologies are common in the heart of radio galaxies, and the observed correlation between jet and disk axes requires a physical connection between these structures over either a small range of orientations (e.g., the cone of avoidance model) or for a subclass of

radio galaxies.

Relativistic effects are known to perturb the inner accretion region, but the spin of a massive Kerr black hole can only strongly affect the orientation of a disk within about ten thousand times the gravitational radius, $r_g = GM_{bh}/c^2 \sim 10^{14}$ cm, where M_{bh} is the mass of the black hole. Outside a few parsecs, Lense-Thirring precession and the associated settling into the midplane, called the Bardeen-Petterson effect, requires longer than a Hubble time to operate (Lense & Thirring 1918; Bardeen & Petterson 1975; Caproni & Abraham 2004; Kumar & Pringle 1985). The precession rate is

$$\Omega_{LT} = \frac{2aG^2M_{bh}^2}{c^3r^3} \quad (1)$$

$$= 7 \times 10^{-16} \text{yr}^{-1} \left(\frac{a}{0.5}\right) \left(\frac{M_{bh}}{10^9 M_\odot}\right)^2 \left(\frac{r}{100 \text{pc}}\right)^{-3}$$

where a is the dimensionless spin parameter. At large radii, the disk is not expected to align with the equatorial plane of the black hole. The inner edge of the disk near $10r_g$ is the proposed site for jet collimation and acceleration (Rees et al. 1982), and most studies predict that the jet should be aligned with the spin axis of the black hole (e.g., Bardeen & Petterson 1975; Kumar & Pringle 1985) but not necessarily the angular momentum of the disk well outside of r_g . A massive spinning black hole can be described as an angular momentum reservoir that varies in momentum, but only very slowly with the influx of fuel. The rate of exchange of angular momentum between the outer disk and black hole is expected to be particularly slow ($\gtrsim 10^9$ years) in radio galaxies where the black holes are massive ($\sim 10^9 M_\odot$) and the fueling rates are low ($\sim 10^{-4} M_\odot \text{yr}^{-1}$, or well below the Eddington rate) (Rees 1978). Thus, the angular momentum of the outer regions of the disk, hundreds of parsecs away from the black hole, is not expected to play a role in aligning the jet axis. The apparent statistical bias toward orthogonal jet/disk orientations therefore presents a mystery. We expect the angular momentum of the very *inner* regions of the disk to couple with the spin of the black hole and the jet axis, but currently there is no

consistent mechanism capable of accounting for jet/disk alignment on 10^2 pc scales.

Noteworthy exceptions to the above generalizations have been considered by a number of studies. A merger of two black holes could change the spin axis of the active galactic nucleus (AGN) on a very short timescale (Merritt & Ekers 2002; Liu 2004). Lubow et al. (2002) showed that when $\beta < h/r$, bending waves may cause the inner disk to be misaligned with the black hole equatorial plane. (Here, β is a dimensionless viscosity parameter, h is the Gaussian scale height, and r is the radius of the disk). Natarajan & Pringle (1998); Scheuer & Feiler (1996) showed that the timescale for a black hole to align with a disk should depend on the ratio between the black hole and disk angular momentum times the Lense-Thirring precession time, rather than an accretion timescale. Quillen & Bower (1999, 1997) showed that the pressure in the ambient interstellar medium (ISM) is sufficiently large to perturb a dusty disk, causing it to precess about the jet axis. Structure associated with radio jets has been clearly revealed in recent observations of the X-ray emitting gas in radio galaxies (e.g., Fabian et al. 2003; Hardcastle, Worrall, & Birkinshaw 1998), implying that there could be a connection between nuclear activity and the energetics of the ISM in radio galaxies and galaxy clusters. The radiative instability proposed by Pringle (1996) could also cause a disk to warp (see also Maloney, Begelman & Pringle 1996).

1.1. The nuclear disk of 3C 449

It is useful to consider radio galaxies for which the jet and disk axes are clearly not orthogonal or are near the cone of avoidance estimated by Schmitt et al. (2002). Specimens possessing extreme (nearly parallel) jet/disk orientations serve as important test cases for physical models capable of coupling the energetics of radio and gaseous structures.

To that end, this paper presents a study of the radio galaxy 3C 449. The elliptical galaxy UGC 12064 is the low redshift ($z = 0.0171$) host to this FR I type radio source, which was imaged with the *Hubble Space Telescope* (*HST*) *WFPC2* camera in the F702W filter centered at $0.7 \mu\text{m}$ (de Koff et al. 2000). Figure 1 (a) reveals a large, ~ 600 pc dusty gas disk with faint spiral features, lying in a plane that is nearly parallel to the jet axis, as seen in Fig. 1 (b). Projected on the sky, the jet axis is at a position angle of $PA \approx 9^\circ$ (Feretti et al. 1999), running nearly north to south, whereas the major axis of the disk has $PA \approx 160^\circ$ (de Koff et al. 2000). As such, the jet/disk angular difference $\Psi_{JD} \approx 29^\circ$, establishing 3C 449 as a counterexample to the jet/disk orthogonality trend proposed by de Koff et al. (2000), being the only FR I radio galaxy (out of 9) to possess dust features with $\Psi_{JD} < 50^\circ$. In the sample discussed by Verdoes Kleijn & de Zeeuw (2005), 6 out of 33 radio galaxies with measured jet/disk position angles have $\Psi_{JD} \lesssim 50^\circ$. For 3C 449, the angle made by the rotational axis of the disk and the jet axis is greater than 60° , placing 3C 449 near the cone of avoidance estimated by Schmitt et al. (2002). 3C 449 is at a distance of 73 Mpc, such that $1''$ corresponds to 350 pc for a Hubble constant of $70 \text{ km s}^{-1} \text{ Mpc}^{-1}$. The maximum angular resolution of the *HST* data is $\sim 0''.1$, corresponding to ~ 35 pc. The mass of the black hole residing at the nucleus of 3C

449 is estimated at $2.5 \times 10^8 M_\odot$ (Bettoni et al. 2003). Based on measurements of the central core at optical, radio and X-ray wavelengths, the active nucleus of 3C 449 has a bolometric luminosity $\sim 10^{42} \text{ erg s}^{-1}$ or $\sim 6 \times 10^{-4}$ of the Eddington luminosity (Donato et al. 2004).

The recent *HST/NICMOS* 3CR snapshot survey (Madrid et al. 2005) allows for a more detailed study of the dust features in UGC 12064. Because extinction from dust is reduced at $1.6 \mu\text{m}$ compared to visible wavelengths, the *NICMOS* image provides a less obscured view of the underlying stellar surface brightness profile. By combining this near-infrared data with the $0.7 \mu\text{m}$ image, we created a colormap which highlights the absorptive features and isocolor contours (isochromes) of the disk. We describe these features in §2, and discuss an observed twist in the isochromes that is inconsistent with the absorptive properties of a planar disk. In §3 we describe our method of creating model images by integrating galactic starlight through an absorptive tilted-ring disk model. We explore non-planar structures for the model disk, finding that a warped geometry provides a possible explanation for the peculiarities observed in the colormap. Our model is used to constrain the morphology of the dusty disk, and in §4 we discuss physical mechanisms which could account for the warp predicted by our model. A summary and discussion follows.

2. OBSERVATIONS

3C 449 has been observed as part of a near-infrared snapshot survey carried out with the *NICMOS* 2 camera on board *HST*, using the F160W broad band filter at $1.6 \mu\text{m}$ (Madrid et al. 2005). After aligning and scaling the images, we created a colormap via division of this data with the $0.7 \mu\text{m}$ image taken with *WFPC2* and previously studied by Martel et al. (2000); de Koff et al. (2000). PSF differences between the two images were ignored, as any variation would only strongly affect regions of high surface brightness, (e.g. near the nucleus). The images and colormap are shown in Figures 1(a), 2, and 4, respectively. A highly inclined, sharply edged disk can be seen in both the 0.7 and $1.6 \mu\text{m}$ images of Fig. 1(a) and 2 and the corresponding colormap (Fig. 4); a structure previously described by Martel et al. (2000); de Koff et al. (2000). The $0.7 \mu\text{m}$ *WFPC2* image reveals more filamentary dust structure than the near-infrared $1.6 \mu\text{m}$ *NICMOS* image. We estimate that the ~ 600 pc disk has an axis ratio of ~ 0.56 near its outer edge, with the $3''.45$ long major axis lying at position angle $PA \sim -20^\circ$.

As expected, absorption from the disk is clearly less prominent at $1.6 \mu\text{m}$ than at $0.7 \mu\text{m}$, so the $1.6 \mu\text{m}$ *NICMOS* image was used to fit a Sérsic surface brightness profile to the galaxy. We use this profile to represent the underlying stellar distribution in our models (see §3). The isophotes at $1.6 \mu\text{m}$ in the central region have ellipticity ranging from 0.1 at a radius of $2''$ to 0.2 at $13''$. As can be seen from the contours in Fig. 3, there is no significant twist in the isophote orientation, as each isophote is aligned with major axis at $PA \approx -10^\circ$.

The major axes of nuclear disks in normal elliptical (Tran et al. 2001) and 3C radio elliptical galaxies (Martel et al. 2000) tend to be aligned within 15° of the galaxy isophotal major axis, and 3C 449 is no exception. The galactic isophotal axis, lying along $\sim -10^\circ$ at radii

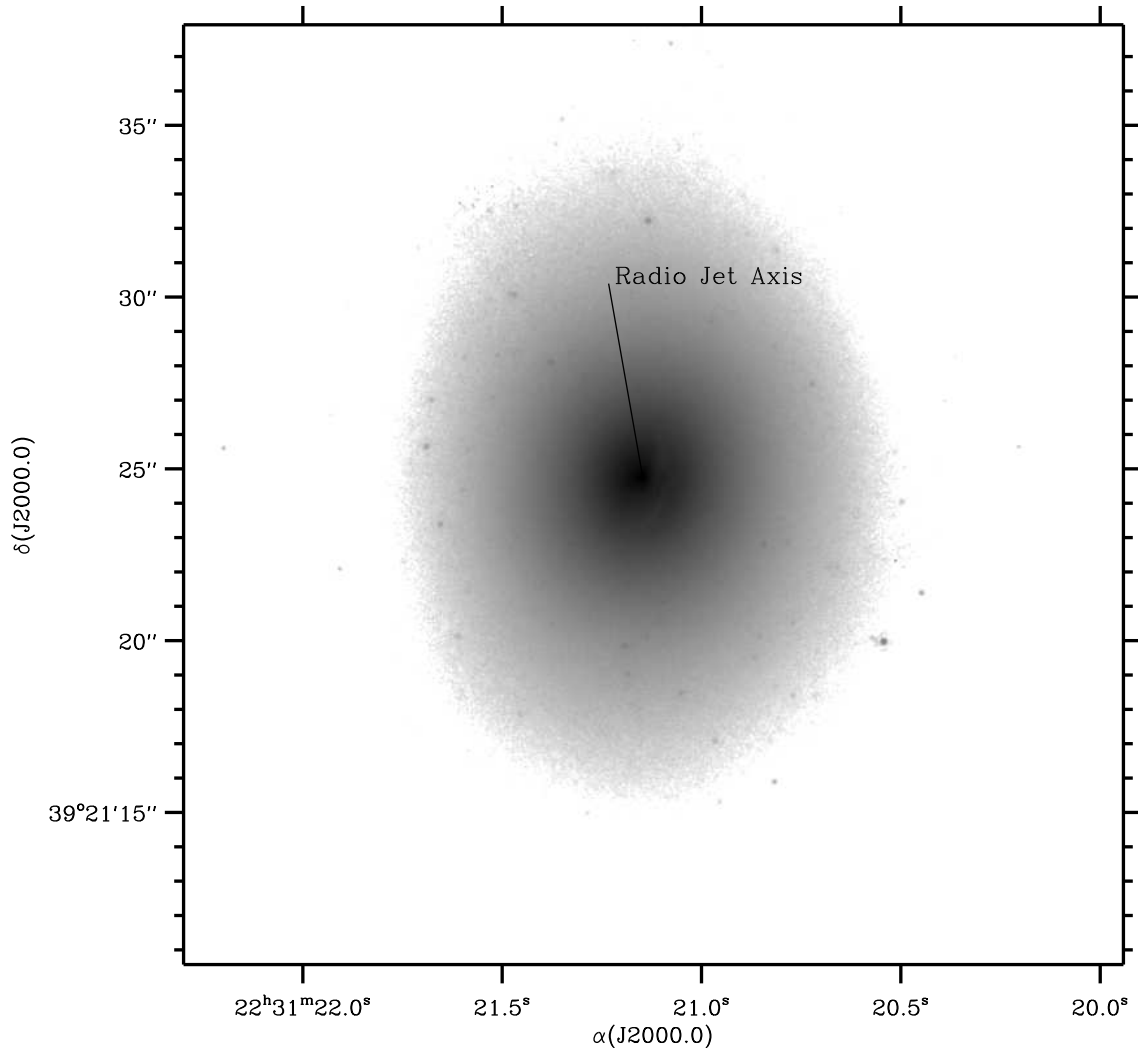


FIG. 2.— *HST/NICMOS* 1.6 μm image of 3C 449. The near side of a dusty torus is seen in absorption on the western side of the nucleus. The jet axis is nearly in the plane of the sky at $PA = 9^\circ$.

just outside the disk (of radius $\sim 2''$), is within 10° of the major axis of the outer edge of the disk, at $\sim -20^\circ$. This suggests that the outer regions of this disk could be dynamically relaxed in the galactic potential.

A closer look at the colormap in Fig. 4 reveals the surprising isochromal properties of the disk. Note how it reddens dramatically from north of the nucleus along the major axis (at $PA \sim 160^\circ$) to the southwestern side, below the nucleus. Even more surprising is the “integral-sign” like twist in the isochromes bordering the southwestern edge of the nucleus. This is unexpected, as a planar absorbing disk should possess elliptical isocolor contours that are aligned with the disk major axis and exhibit reflective symmetry about the disk minor axis. This is not the case in the colormap of 3C 449.

Note the linear streaks along the disk in the colormap, which have been described as spiral arms or dusty filaments by previous studies (de Koff et al. 2000; Martel et al. 2000). Near the nucleus, linear dust filaments are tilted at an angle more nearly east-west than in the outer disk. At a radius of $0''.2$ the linear dust fea-

tures are at a shallow position angle of $\sim 110^\circ$, whereas near the edge of the disk, the features are nearly aligned with the disk edge at $PA \sim 160^\circ$. For a planar disk, one would expect tightly wound spiral features to cause dark absorption lanes that are approximately parallel to the outer disk edge at all radii. However, if the spiral spiral features are more open (less tightly wound) near the nucleus they may cause a shift in the observed position angles of the features.

The isophotes in the 1.6 μm image of Fig. 3 are nearly round in front of the disk (to the northeast), so there is no evidence that the stellar distribution is lop-sided or barred. The disk outer edge has nearly the same major axis as the galaxy isophotes. Outside regions where there is strong extinction from the disk, we see no significant twist in the position angle of the galaxy isophotes as a function of radius. Thus, we have no reason to suspect that the galaxy is strongly triaxial in its central kpc-scale regions. A stellar bar with a major axis of $3''$ - $4''$ would be capable of causing a twist in colormap isochromes, but a bar that is sufficiently triaxial to account for such a

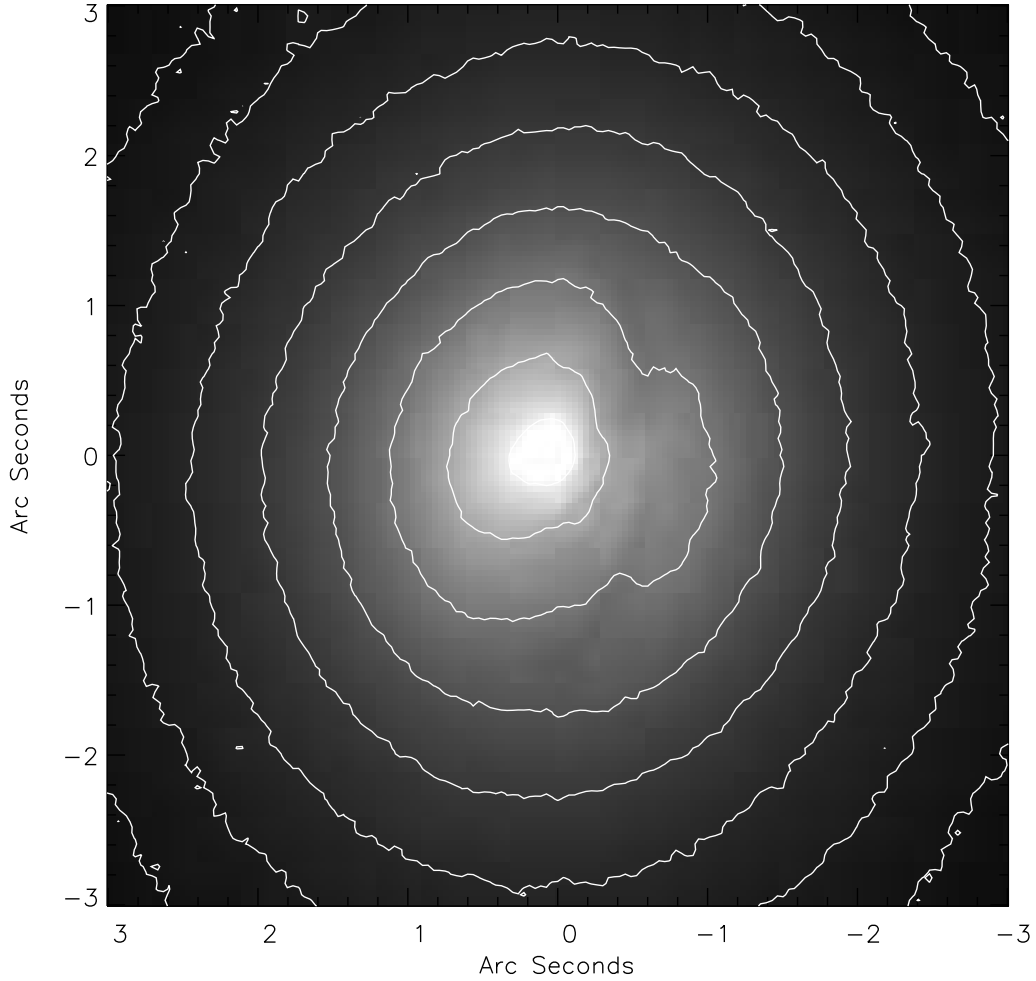


FIG. 3.— *HST/NICMOS* 1.6 μm image of 3C 449 with contours marking isophotes. The contours highlight every 0.4 magnitude difference in brightness, moving outward from the core. The innermost contour marks a brightness of 13.7 *H*-band magnitudes per square arcsecond. Note that the major axis of each contour is generally aligned with all others, suggesting that the galaxy is unlikely to be triaxial.

twist would likely need to rotate to be stable. A rotating bar generally truncates sharply near its corotation radius. The surface brightness profile on the northeast side is smooth (and well fit by a Sérsic profile), so it is unlikely that the stellar distribution is strongly triaxial (rotating or otherwise) in the central few arcseconds from the nucleus. As such, the twist observed in the colormap is most likely caused by the disk itself, rather than a projection effect from a strongly triaxial nuclear cusp.

This motivates the creation of an absorptive numerical model for the disk and underlying starlight distribution. In §3 we explore warped geometries for the disk in an attempt to reproduce the isochrome twist seen in Fig. 4, and constrain the geometry of the disk accordingly.

3. A NUMERICAL WARPED DISK MODEL FOR 3C 449

We now describe our procedure for creating an absorptive tilted-ring model of the gas disk of 3C 449. The starlight from behind the disk is integrated, multiplied by an absorption factor due to the disk and added to the integrated starlight from in front of the disk. To create such a model, we require a light density function and a geometric model for the disk which specifies its opacity

as a function of position on the sky and its position along the line of sight in the galaxy.

We describe the stellar luminosity density $\rho(s)$ where $s = \sqrt{(1 - e_g^2)r^2 + z^2}$. The ellipticity of the galaxy, e_g , was not allowed to vary with radius. Our function for $\rho(s)$ is consistent with the Sérsic law, fit to the surface brightness profile of the *NICMOS* image using the routine *GALFIT* (Peng et al. 2002). The galactic surface brightness profile is

$$I(s) = \exp \left[-b_n \left(\frac{s}{s_0} \right)^{\frac{1}{n}} \right] \quad (2)$$

where the scale length s_0 and power n are listed in Table 1; (for $n = 4$ a de Vaucouleur law is recovered). Here $b_n = 2n - \frac{1}{3} + \frac{0.009876}{n}$, as approximated by Prugniel & Simien (1997).

The light density from stars (in 3 dimensions) that is consistent with the Sérsic surface brightness profile is given by Prugniel & Simien (1997),

$$\rho(s) = s^{-\alpha_r} \exp \left[-b_n \left(\frac{s}{s_0} \right)^{\frac{1}{n}} \right] \quad (3)$$

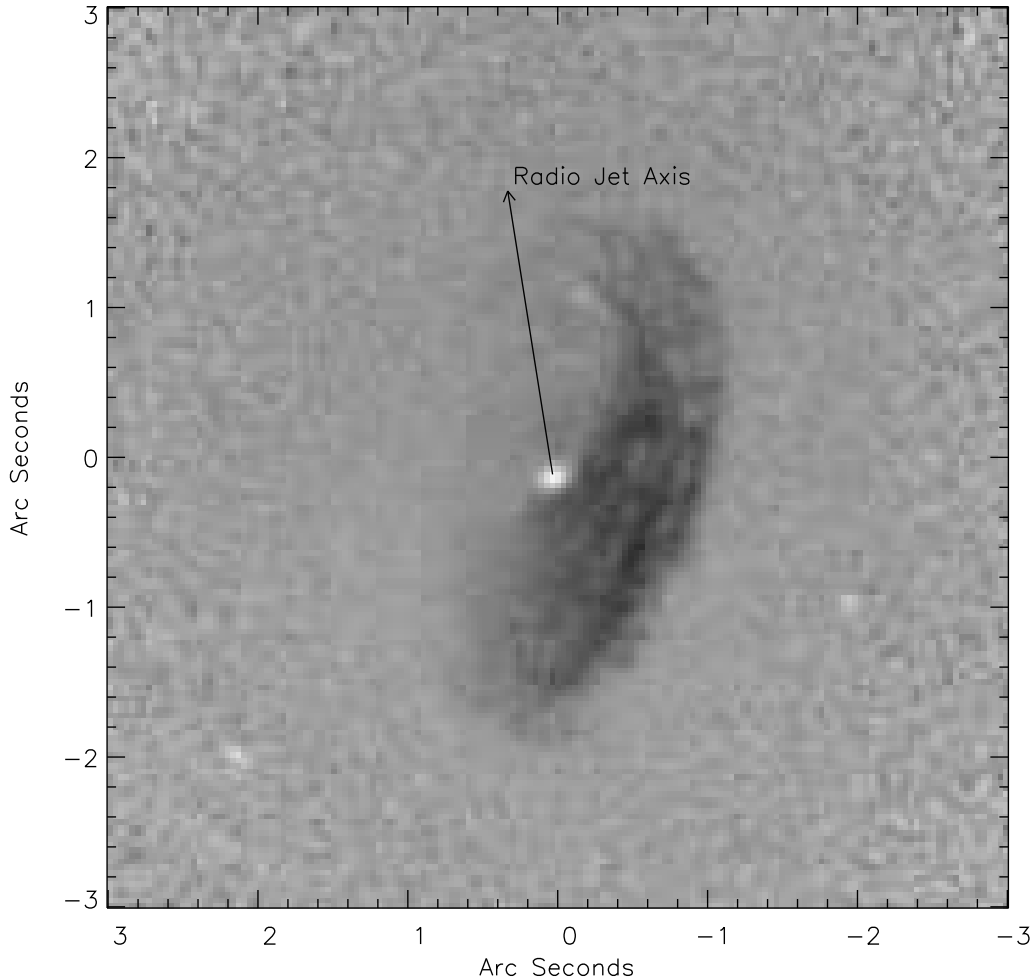


FIG. 4.— Colormap of 3C 449 generated via division of the $1.6\ \mu\text{m}$ *HST NICMOS* image by the *WFPC2* image at $0.7\ \mu\text{m}$. Note the reddening of the disk south of the nucleus. There is approximately a 0.5 magnitude difference between the faintest and brightest portions of the colormap. The radio jet axis is at a position angle of 9° , measured north through east. Note the misalignment of the isochromes, particularly the “integral-sign” like twist in those bordering the southwestern side of the nucleus. A planar disk should exhibit isochromes that are aligned with the disk major axis at all radii, which is clearly not the case for this object.

where α_r is a free parameter well approximated with the expansion $\alpha_r = 1.0 - \frac{1.188}{2n} + \frac{0.22}{4n^2}$. We checked that this density function provides a good match to the surface brightness profile by comparing the model light, generated from Eq. 3 and integrated along the line of sight, with the surface brightness profile at $1.6\ \mu\text{m}$ and the Sérsic function that was fit to it.

The dusty disk is assumed to be comprised of a series of rings of radius r , each with an orientation described by two parameters: a tilt with respect to the line of sight, $\omega(r)$, and $\alpha(r)$, the position angle from north on the sky. We have defined these angles with respect to the line of sight, not with respect to the galactic midplane or the jet axis. We assume that $\omega(r)$ and $\alpha(r)$ are powers of r , such that $\omega(r) \propto r^{a_\omega}$ and $\alpha(r) \propto r^{a_\alpha}$. The opacity of the disk (if viewed face-on) is described by $\tau(r) \propto r^{a_\tau}$. We specify the angles and opacity at two radii, r_{\min} and r_{\max} . We assume that interior and exterior to these radii the disk opacity is zero.

We create two arrays, with coordinates x, y corresponding to positions on the sky. The first array con-

tains the opacity of the disk at this position; the second contains the location of the disk along the line of sight. Our numerical procedure begins with a random selection of points r, θ in the disk. Using the ring orientation functions $\alpha(r)$ and $\omega(r)$, the position of this point is projected to determine x, y on the sky and z along the line of sight. The disk opacity is computed from the radius, and stored along with the vertical position of the disk in the two arrays described above.

At each position on the sky, light from the galaxy is integrated using the stellar luminosity density $\rho(s)$ from $-\infty$ to the disk surface (with position stored in the second array). The sum of light from behind the disk is multiplied by $e^{-\tau}$ at that position (from the other array) to take into account absorption by the disk. This flux is then added to the integrated star light in front of the disk (from $+\infty$ to the disk surface). The opacity at $0.7\ \mu\text{m}$ of the dusty disk is assumed to be 4.16 times that at $1.6\ \mu\text{m}$, consistent with a galactic extinction law (Mathis 1990). The output of the light density integration produces model images at $0.7\ \mu\text{m}$ and $1.6\ \mu\text{m}$. As was the

TABLE 1
PARAMETERS FOR WARP MODEL

Parameter	Value	Comments
Isophotal Parameters		
n	1.2797	From <i>GALFIT</i>
s_0	5''.6625	From <i>GALFIT</i>
e_g	0.175	From <i>GALFIT</i>
Opacity Parameters		
r_{min}	0''.1	Minimum <i>HST</i> resolution
r_{max}	1''.6	Estimated from Fig. 4
τ_{min}	0.04	Estimated opacity at r_{min}
τ_{max}	0.09	Estimated opacity at r_{max}
a_τ	1.0	For $\tau(r) \propto r^{a_\tau}$
Warp Parameters		
ω_{min}	-10°	Disk inclination at r_{min}
ω_{max}	-23°	Disk inclination at r_{max}
α_ω	1.0	For $\omega(r) \propto r^{\alpha_\omega}$
α_{min}	-73°	PA of disk at r_{min}
α_{max}	-14°	PA of disk at r_{max}
α_α	1.0	For $\alpha(r) \propto r^{\alpha_\alpha}$

NOTE. — Isophotal parameters are from *GALFIT* (Peng et al. 2002). Angles for α are position angles (PA), measured from north through east on the sky (counterclockwise). ω is a tilt with respect to the line of sight ($\omega = 0^\circ$ for edge on disk). A negative angle for ω means that the southern edge of the disk is the near side. The jet axis is assumed to be in the plane of the sky and at $PA = 9^\circ$.

case for the *HST* data, we create a model colormap via division of these two output images.

3.1. Comparison of model and galaxy images

Our goal in creating models is to test the hypothesis that the disk of 3C 449 is warped, and to better constrain the geometry of the disk. We alter model parameters to obtain a qualitative match to the morphology of both the colormap and the $1.6 \mu\text{m}$ image. Our best matching model, shown in Fig. 5, compares the image at $1.6 \mu\text{m}$ to the model image, and Fig. 6 shows the colormap compared to the model as viewed in $1.6 \mu\text{m}/0.7 \mu\text{m}$. The parameters for this model are listed in Table 1.

Figures 5 and 6 illustrate that a warped disk model is successful in reproducing the appearance of the *HST* images. Specifically, we find that absorption in a non-planar disk can give rise to an “integral-sign” like twist in isochromes, as is observed in the colormap of 3C 449. The model also successfully exhibits absorption along the western edge of the disk in the $1.6 \mu\text{m}$ image. In *H*-band, light from behind the disk is absorbed by the southwestern (nearest) side, but is visible past the edge. The same is true for the representative model, which differs from the *NICMOS* image in that the far side of the disk is also visible and appears larger. This is due to extinction effects leading to obscuration of the disk at $1.6 \mu\text{m}$. The colormap reveals the underlying morphology of the absorptive dust features, so it was used as the basis for shaping our model disk. Because our model lacks azimuthal (non-radial) density variations or spiral surface features, it cannot reproduce the linear streaks seen in

absorption in the $1.6 \mu\text{m}$ *NICMOS* image.

Fig. 6 is more convincing, as it shows that our model can reproduce the “integral sign” twist in the isocolor contours near the nucleus of the colormap, as well as match the shape of the absorptive features quite well, particularly on the southwestern edge of the disk.

Certainty and degeneracy in model parameters is of key importance in judging the qualitative success of the model. We first list the parameters that were held fixed and then describe those that we varied to find a model that best matched the images. The isophotal parameters n and s_0 were fixed since they are consistent with the Sérsic law fit to the surface brightness profile of the galaxy. We fixed the galaxy ellipticity e_g at 0.175, as this produces model isophotes that are sufficiently oblate to be consistent with the isophotal ellipticity at $1.6 \mu\text{m}$. We set the maximum radius of the disk to match that of the outer disk edge, $r_{max} = 1''.6$. Likewise the tilt, $\omega_{max} = -23^\circ$ (w.r.t. the line of sight), and position angle, $\alpha_{max} = -14^\circ$, of the outermost ring (at radius r_{max}) were fixed and set to be consistent with the location of the disk’s outer edge. The inner model ring was set with $r_{min} = 0''.1$, corresponding to the maximum angular resolution of *HST*. We cannot probe the geometry of the disk at radii smaller than this, so this radius does not describe an inner edge for the disk. Rather, it is used to provide boundary conditions for the positional functions $\alpha(r)$ and $\omega(r)$, and for the opacity function $\tau(r)$.

The model is strongly sensitive to changes in the optical depth of the disk, which is set by the parameters τ_{min} and τ_{max} at the innermost and outermost rings, and with an exponent, a_τ . Such sensitivity allows us to constrain the opacity parameters by incrementally altering τ_{min} and τ_{max} until the isophotes of the model colormap match the images. Too high an opacity leads to overly strong absorptive features not observed in the *NICMOS* image, and opacity endpoints that are too low have the opposite effect. The best match for our model was in the range of *R*-band opacity $\tau_{min} = 0.04 \pm 0.02$ to $\tau_{max} = 0.09 \pm 0.02$. This physically reasonable *R*-band opacity range generates isochromes that match those seen in the *HST* colormap. Still, there is inherent uncertainty in our values for these parameters, as their effects on the absorptive features differ depending on the shape of the disk. A disk of constant density has a higher opacity when viewed at high inclination than when viewed face-on. Thus, there is a larger range of values over which the inner ring opacity will produce an “integral-sign” twist. This, along with the orientation of the inner ring, is the greatest source of uncertainty in our model.

The model is not as sensitive to the exponent a_τ in the power law $\tau(r) \propto r^{a_\tau}$. While opacity and ring orientation effect the structure of the model isochromes, a_τ effects how steeply an absorptive feature tapers off as a function of radius. This dependence is minimal, in that a model with $a_\tau = 0.5$ and a model with $a_\tau = 1.5$ will produce similar results, both of which closely resemble the data if the positional parameters and opacity boundary conditions are set appropriately. As such, a_τ is only loosely constrained, and we set it to $a_\tau = 1.0$ as it generates absorptive features in the model colormap that are consistent with those seen in the data.

While the strength of the absorptive features is mostly

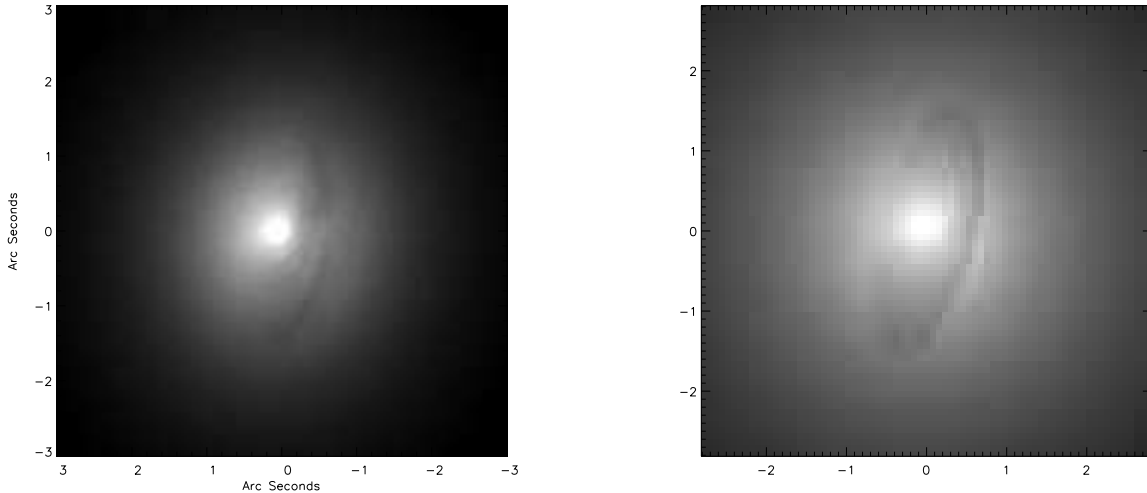


FIG. 5.— Comparison of a) $1.6\ \mu\text{m}$ *NICMOS* image with b) the $1.6\ \mu\text{m}$ integrated light warped disk model. Note the similar absorptive properties of both the disk and its numerical representation. The disk in the model image appears larger than that in the *NICMOS* data as extinction from the galaxy masks the outer regions of the disk at $1.6\ \mu\text{m}$. In our model, we do not take into account extinction from the surrounding galaxy. The integrated light density function used in creating the model is based upon isophotal analysis of the *NICMOS* image. The *R*-band opacity drop-off ~ 0.05 follows a simple power law in an attempt to obtain a qualitative match to the data (see §3). Model parameters are listed in Table 1.

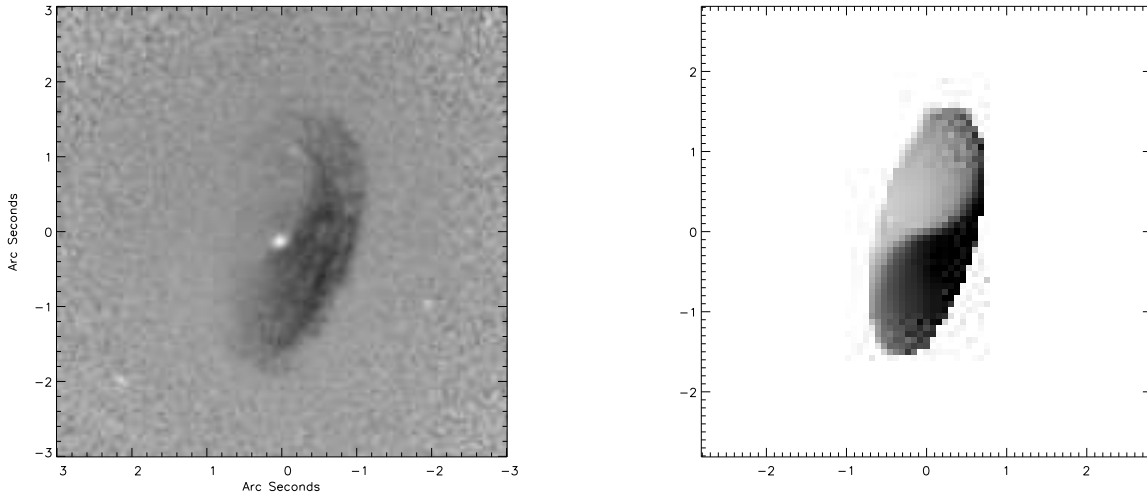


FIG. 6.— Comparison of a) colormap of 3C 449, generated via division of the $1.6\ \mu\text{m}$ and $0.7\ \mu\text{m}$ *HST* images, with b) the model colormap. Note the successful reproduction of the isochrome twist to the north of the nucleus. Our model assumes that the disk is warped but featureless, so the spiral features are not seen in the model. Model parameters are listed in Table 1.

dependent upon $\tau(r)$, isochrome *shape* most strongly depends on the structure of the disk. Qualitatively, one can achieve similar outer disk appearances by raising α and decreasing ω (or vice-versa). Being concerned only with the appearance of the disk, the small range over which α and ω are degenerate is of little relevance. The orientation of the innermost ring is of particular interest, since it is located only ~ 30 pc from the nucleus. The best matching model exhibits a dramatic warp, with the inner ring at a radius of $0''.1$ at a position angle of $\alpha_{min} = PA = -73^\circ$. We estimate the best fit for the tilt of the inner ring is at $\omega_{min} = -10^\circ$ w.r.t. the line of sight.

Remarkably, the best matching model is such that the inner regions of the disk are nearly perpendicular to the jet axis. Assuming the jet axis is orthogonal to the line

of sight (e.g., in the plane of the sky) and at $PA = 9^\circ$, the axis of symmetry of the innermost model ring makes a 3D cone angle with the jet axis of approximately 10° , meaning the inner regions of the disk are within 10° of being orthogonal to the jet axis. The uncertainty brought about by the codependence of α and ω on disk appearance is small enough such that we can be fairly certain of this value, as all “good-fit” models have inner rings nearly perpendicular to the jet axis. Consequently, our model shows that 3C 449 may actually *conform* to the trend proposed by previous studies suggesting that dusty disk major axes are preferentially oriented nearly perpendicular to jet axes on the sky (de Koff et al. 2000; van Dokkum & Franx 1995; Sparks et al. 2000).

3.2. Comparison of warp model to observations at other wavelengths

The success of the non-planar model in reproducing the observed isochrome twist in 3C 449 leads us to suspect that the dust disk is warped between a radius of ~ 50 pc (the innermost radius we can easily resolve) and 600 pc (the disk outer edge). We now discuss the geometry and orientation of the dusty disk in context with observations of the nuclear region at other wavelengths.

Martel et al. (2000) presented narrow band images of 3C 449 in $\text{H}\alpha + \text{N[II]}$, showing stronger emission to the north of the nucleus. Likewise, the near-UV image presented by Allen et al. (2002) showed similar morphology with brighter near-UV emission to the north of the nucleus. The UV image exhibits arm-like features that are bounded by dusty absorptive streaks also present in the visible band image (as discussed by Allen et al. 2002).

Because extinction is deep along the disk edge to the west of the nucleus, we infer that the western side of the disk is nearer to us than the eastern side. Studies of the radio emission have suggested that the jets are nearly in the plane of the sky, at approximately 70° from the line of sight, with the southern side nearer the observer (Gower & Hutchings 1982). As such, we expect that the northern jet is in front of the disk and the southern jet is behind. The UV emission might be excited by star formation in the disk (e.g., O’Dea et al. 2001, in the case of 3C 236), or it might be related to shocks or illumination along the jet axis (e.g., Solrzano-Iarrea et al. 2002). Since bright UV or $\text{H}\alpha + [\text{NII}]$ emission is not seen on the southern side or along the western disk edge, the emission probably does not arise from material embedded in the disk. If the emission is from a large diffuse region (possibly wide cones) above and below the disk and oriented approximately along the jet axis, the emission from southern side should suffer more extinction from the disk. Previous studies (e.g., Quillen et al. 1999) have found that structure in an ionization cone can be related to the underlying dust distribution in the galaxy. However, the UV emission from 3C 449 is brighter outside the dusty features than on top of them, though UV emission is also brighter in proximity to dust features, so the presence of dense material may somehow contribute to the excitation. The morphology of the UV emission would be difficult to account for with a simple model, but excitation along a wide cone associated with the jet axis and coupled with extinction from the dusty disk might be consistent with the observed morphology, so long as the UV emission were stronger in proximity to dust features. The UV emission also exhibits a deficit (or perhaps a shadow) just north of the nucleus. Our model does not include material that could absorb UV emission in this location, but a warped disk that continues to twist past our observational limit at r_{\min} could possibly account for such a shadow.

We can consider the possibility that blue continuum emission associated with the UV structure could have reduced the redness of color to the north of the nucleus, accounting for the observed isochromal twist in the colormap. If this were so, we would predict that the size and location of features seen in the UV image would correspond to blue regions in our color map. The colormap is quite smooth, whereas the UV emission is clumpy. Fur-

thermore, bright UV emission is offset from the spiral features seen in absorption. This would make it impossible for a blue continuum associated with the UV emission to cancel out the extinction associated with dust lanes.

3.3. Comparison to Spectra

Our warp model predicts that the inner disk (at $r \sim 100$ pc or $0''.3$) is nearly edge-on and oriented almost directly east-west, whereas the outer disk at $r \sim 600$ pc is oriented with major axis oriented approximately north-south. We can compare this prediction to spectroscopic observations that measure the mean velocity of the ionized gas. Noel-Storr et al. (2003) obtained spectra with *STIS* on board *HST* along 3 slits oriented at a position angle of 170.6° (approximately north-south along the major axis of the outer disk). Mean velocities measured along these slits are presented in Figure 22 and Table 26 of Noel-Storr et al. (2003). The mean velocity $\sim 0''.5$ north of the nucleus is ~ 400 km/s above that $\sim 0''.5$ south of the nucleus. The observed velocity profile along the outer disk major axis is consistent with a rotating disk that is approaching the observer on the northern side and receding on the southern side. The warp model predicts that the eastern side of the inner disk should have radial velocity with the same sign as the southern side of the outer disk. Because the southern side of the outer disk is receding from us, our model implies that the eastern side of the inner disk should be receding, while the western side should be approaching the observer.

Mean velocities were also measured in the two slits $\pm 0''.1$ from the nucleus and parallel to the central (nuclear) slit. Velocities along the east-west direction can be used to test the sign of the rotation predicted by the model. The velocities on either side (east and west) of the nucleus are lower and higher (respectively) than the systemic velocity, suggesting that the velocity field is twisted. East of the nucleus, Noel-Storr et al. (2003) found the velocity to be sub-systemic. To the west, a velocity consistent with that observed along the major axis south of the nucleus was measured. This would be consistent with a disk that is rotating such that southern and eastern sides of the outer disk are receding from the observer. We find that the sign of the velocities along the east-west direction is consistent with the prediction of our warped disk model.

4. MECHANISMS FOR CAUSING THE WARP

We have shown that a warped disk could account for the twist in the isochromes seen in the dusty disk of 3C 449, and that our model is consistent with observations at other wavelengths. With an outer edge at $r \sim 600$ pc, the disk is approximately in the midplane of the galaxy and tilted about 30° away from the jet axis. If our model is correct, at smaller radii (~ 100 pc), the disk is nearly orthogonal to the jet. Verdoes Kleijn & de Zeeuw (2005) outlined two scenarios that could account for such a jet/disk orientation.

1. The disk is initially planar and sets the jet axis. At later times the disk is affected by the torque from the galaxy and becomes aligned with the galaxy isophotes.
2. Another force, possibly aligned with the jets, pushes on the disk, twisting it at small radii.

Might the morphology of the disk in 3C 449 discriminate between these two scenarios? We can consider a gas disk to be comprised of rings moving in nearly circular motion. When the galaxy is non-spherical, it exerts a torque on each ring causing precession about a galactic axis of symmetry. The precession rate is $\dot{\alpha} \sim \Omega \epsilon_{\Phi}$ where Ω is the angular rotation rate of a particle in a circular orbit and ϵ_{Φ} is the ellipticity of the galactic gravitational potential. (Here α refers to a precession angle which is measured with respect to a principal plane of the galaxy). The precession rate is primarily set by Ω , and so depends on the rotation period at a given radius, $P = 2\pi/\Omega$. Since the rotation period is shorter at smaller radii, the inner disk should be more twisted than the outer disk, unless the galaxy ellipticity drops rapidly near its inner regions. Such a drop in ellipticity is not seen in the isophotes of Fig. 3, though the presence of the disk itself does not make this absolutely certain. As the disk becomes increasingly twisted, the inner region can settle into the galactic midplane (e.g., Steiman-Cameron & Durisen 1988) with the outer disk warped and misaligned with the galaxy. Instead, we find that the *outer* part of the galaxy is settled into the midplane and the *inner* part deviates from or is inclined with respect to this plane. This is not consistent with the first scenario discussed above. The morphology of the disk instead suggests that it was once relaxed in the symmetry plane and subsequently perturbed by a force from the nucleus, pushing the inner disk out of alignment on a small, ~ 100 pc scale.

We now consider candidate scenarios which could account for such a warp:

1. Precession in the inner disk has been induced by a binary massive black hole.
2. Radiation pressure from the central source has twisted the disk. The inner disk may have become warped via a self-induced radiation-driven mechanism (Pringle 1996).
3. There is strong coupling between the outer disk and the inner disk, aligned by the Bardeen-Peterson effect with the spin of the black hole (Natarajan & Pringle 1998; Scheuer & Feiler 1996).
4. A jet-excited ambient interstellar medium has perturbed the disk. This would be a form of feedback from an AGN.

We discuss these scenarios below.

4.1. Precession due to a binary black hole

It is useful to summarize bulge and black hole properties for 3C 449. Bettoni et al. (2003) have listed a bulge velocity dispersion of 225 km s^{-1} and estimated a black hole mass of $2.5 \times 10^8 M_{\odot}$. A transition radius (e.g., the sphere of influence) where the gravitational force from the nuclear black hole dominates that from the bulge is

$$r_t = \frac{GM_{bh}}{2\sigma_*^2} = 10 \text{ pc} \left(\frac{M_{bh}}{2.5 \times 10^8 M_{\odot}} \right) \left(\frac{225 \text{ km/s}}{\sigma_*} \right)^2 \quad (4)$$

Note that the transition radius can be compared to the semi-major axis for a possible black hole binary which

makes it “hard”

$$a_{hard} < \frac{G\mu}{4\sigma_*^2} = r_t \frac{\mu}{2M_{bh}}, \quad (5)$$

where μ is the reduced mass of the black hole binary and M_{bh} now represents the sum of the two black hole masses (Caproni & Abraham 2004). For an equal mass binary $a_{hard} = r_t/4 \sim$ a few pc for 3C 449.

We consider a disk exterior to a binary black hole in a circular orbit with semi-major axis a_b and reduced mass μ . At radius $r > a$, the binary black hole exerts a quadrupolar perturbation on the gravitational potential

$$\Phi_2 = \frac{3G\mu a_b^2 z^2}{r^5}. \quad (6)$$

The vertical oscillation frequency is estimated by differentiating Φ_2 twice with respect to z , and adding it to that from the spherical component from the galaxy,

$$\nu \sim \Omega \left[1 + \frac{3\mu}{M(r)} \left(\frac{a_b}{r} \right)^2 \right], \quad (7)$$

where $M(r)$ is the total mass within radius r . The precession rate is

$$\dot{\delta} = \nu - \Omega \sim \Omega \left(\frac{3\mu}{M(r)} \right) \left(\frac{a_b}{r} \right)^2. \quad (8)$$

Relating $M(r)$ to the velocity of a particle in a circular orbit, we have $M(r) = v_c^2 r / G$. Outside the black hole sphere of influence, we expect $M(r) \propto r$, and $\Omega \propto r^{-1}$, consistent with a flat rotation curve, such that $\dot{\alpha} \propto r^{-4}$. The precession period is then

$$P_{\delta} \sim 10^{10} \text{ yr} \left(\frac{\mu}{10^8 M_{\odot}} \right)^{-1} \left(\frac{r}{100 \text{ pc}} \right)^4 \left(\frac{a_b}{1 \text{ pc}} \right)^{-2} \left(\frac{v_c}{320 \text{ km/s}} \right). \quad (9)$$

(For an isothermal sphere $v_c \sim \sqrt{2}\sigma_*$.)

Such a long timescale and steep dependence on radius presents a problem for this scenario. For a binary black hole semi-major axis larger than a few pc, dynamical friction can bring the black holes together on a timescale of order a few times the rotation period. Only if the black hole binary is hard ($a_b \lesssim$ a few pc) can the black hole separation shrink slowly, within a timescale on the order of a Hubble time (e.g., Milosavljevic & Merritt 2003). If the black hole binary is not hard, then it would spiral inward too fast to create the warp. We find that the estimated precession timescale is too long to account for the warp in the disk.

One might consider alternative models where the disk precessed while a secondary black hole spiraled inward. Since the black hole orbit need not be planar, it could account for a highly warped geometry in the disk. In this case, however, one would expect to see disturbed material on both large and small scales. Other than the active nucleus, the galaxy appears dynamically relaxed, and there is little evidence for a recent galactic merger in its isophotal structure (see Fig. 3).

4.2. Radiative Warp Instability

Here we explore the proposal by Pringle (1996); Maloney, Begelman & Pringle (1996) that the absorption of radiation from a central source can cause a surrounding disk to precess and warp. The precession rate can be estimated from the constant torque solution of Maloney, Begelman & Pringle (1996) (their equation 8), giving a precession period of

$$P_{RW} = \frac{48\pi^2 \Sigma r^2 v_c c}{L_{bol}} \quad (10)$$

where Σ is the disk mass surface density, and L_{bol} is the bolometric luminosity of the central source. Inserting values appropriate for 3C 449, we estimate a precession period

$$P_{RW} = 9 \times 10^{10} \text{ years} \left(\frac{v_c}{330 \text{ km/s}} \right) \left(\frac{\Sigma}{1 M_\odot / \text{pc}^2} \right) \left(\frac{L_{bol}}{10^{42} \text{ erg/s}} \right)^{-1} \left(\frac{r}{100 \text{ pc}} \right)^2. \quad (11)$$

The values used are based on the following estimates: The radio core luminosity at 5 GHz is lower than that estimated from an unresolved source in the nucleus at optical wavelengths, with a luminosity of $\sim 10^{40.8}$ erg/s (Chiaberge et al. 1999; Capetti et al. 2002), and at X-ray wavelengths with a luminosity of $\sim 10^{41}$ erg/s (Donato et al. 2004). The total bolometric luminosity from the core is estimated to be 10 times that in X-ray, or $L_{bol} \sim 10^{42}$ erg/s (Donato et al. 2004). Assuming constant *R*-band opacity for a face on disk of 0.065, we use the extinction coefficients in Mathis (1990) and estimate the surface mass density in the disk to be $\Sigma \approx 1.3 M_\odot \text{ pc}^{-2}$. The circular velocity $v_c \sim 330 \text{ km/s}$ is estimated from the velocity dispersion listed by Bettoni et al. (2003), assuming an isothermal sphere.

A quarter precession period would be long enough to account for the extent of the warp in 3C 449, and this would reduce the above timescale by a factor of a few. Even so, this reduced timescale is still very long, so this model is not likely responsible for the warp. The precession rate might have been faster if the luminosity were significantly higher in the past. However, there should also be a corresponding increase in the surface density of the disk, consistent with the higher rate of accretion. We conclude that precession due to radiation pressure from a central source is probably too slow to generate the warp. The growth time for the radiative warp instability is approximately the same as the above period divided by the order of the mode grown. However, the observed warp is large-scale (with wavevector similar to the radius), so a higher order mode is unlikely to account for it. This finding is consistent with a similar estimate by Ferrarese & Ford (1999), for the warped disk in NGC 6251.

4.3. Quick Disk/Black Hole Alignment

Scheuer & Feiler (1996); Natarajan & Pringle (1998) showed that a black hole could align with a disk on a timescale set by the ratio of the black hole and disk angular momentum times the Lense-Thirring precession period. The Lense-Thirring precession period is $\propto r^3$ and the disk angular momentum is $\propto r$, so the timescale for alignment becomes very long at distant radii. The ratio

of the black hole angular momentum to the disk angular momentum is not small enough to reduce the alignment timescale at 100 pc to a level that would allow alignment to take place within a Hubble time (see the Lense-Thirring precession rate given above in Equation 2). We can therefore reject this scenario based on these simple timescale estimates.

4.4. Disk-ISM interaction

If the pressure gradient from the ambient ISM across the disk is large, it can overcome the torque from the galaxy (Quillen & Bower 1999, 1997). The pressure required to keep a disk of surface mass density Σ from precessing in a galaxy of ellipticity ϵ_Φ is

$$P_\tau \gtrsim 2 \times 10^{-11} \text{ dynes cm}^{-2} \left(\frac{\epsilon_\Phi}{0.05} \right) \left(\frac{\Sigma}{1 M_\odot / \text{pc}^2} \right) \left(\frac{v_c}{330 \text{ km/s}} \right)^2 \left(\frac{100 \text{ pc}}{r} \right) \cos(\theta_g) \sin(\theta_g) \quad (12)$$

where θ_g is the disk inclination angle (with respect to the galaxy axis) (Quillen & Bower 1999).

Hardcastle, Worrall, & Birkinshaw (1998) observed that the X-ray emission in 3C 449 on arcminute scales was anisotropic, with isophotes aligned orthogonally to the jet axis, suggesting that there is a deficit of X-ray emission near the radio lobes. The central gas density is $\sim 4.6 \times 10^{-3} \text{ cm}^{-3}$, temperature $kT = 1.2 \text{ keV}$, and central pressure of $10^{-12} \text{ Pa} = 10^{-11} \text{ dyne cm}^{-2}$ at a radius of about 0.5 arcminute. Consequently the pressure at a radius of few arcseconds from the nucleus could be a factor of 10 or so higher, or $\sim 10^{-10} \text{ dyne cm}^{-2}$. A comparison between this number and the relation of Eqn. 12 shows that the pressure in the X-ray emitting ISM is large enough to perturb the gas disk on reasonable timescales, so long as the isobars of X-ray emitting gas in the ISM are very elongated, structured, and anisotropically distributed.

Quillen & Bower (1999) explored a simplistic model in which the ambient ISM has isobars elongated along the jet axis. In this case, the ISM exerts a torque on the disk, and gives rise to precession about the jet axis. However, if our model is correct, the disk in 3C 449 passes smoothly from the galaxy midplane at its outer edge to the plane perpendicular to the jet. If the jet causes a wind, the disk would be lifted out of the plane perpendicular to the jets, rather than pushed into it (e.g., Quillen 2001). Similarly, an azimuthal pressure variation across the disk may overcome the influence of the galaxy potential and perturb the disk at 100 pc, though not in ways capable of creating the warp we predict exists in 3C 449. As discussed by Quillen & Bower (1999), gas isobars initially aligned with the jet should align with the galaxy equipotentials on a sound crossing time, of order the rotation period at 100 pc (a few Myr). Therefore the torque on the disk provided by static gas pressure in the ISM, no matter how strong or non-axisymmetric, could only cause the disk to precess and eventually settle into the galactic midplane, and not the plane perpendicular to the jets. The precessing disk may be damped via internal kinematics (e.g., high viscosity, collisions, etc.), but the time associated with the damping would be of order the accretion timescale, which is too long to account for the warp. Even if the region is ram pressure dominated

and the gas in the disk is stirred near the sound speed, the azimuthal pressure gradient required to warp the disk would be unrealistically large. The Quillen & Bower (1999) model is therefore incapable of explaining the existence of the warp in 3C 449. That study, however, did not take into account the emergence of *Chandra* observations revealing temperature fluctuations and buoyant bubbles in the X-ray emitting ISM surrounding an AGN (e.g., Fabian et al. 2003). Such structure in the region is likely associated with the jet lobes, responsible for injecting large amounts of energy and momentum into the ambient medium. A drag force between jet-excited bubbles and the disk would not give rise to an instability (as explored by Quillen 2001), and the warp would be damped. The inner disk could thus be pushed into the plane perpendicular to the jet. If the UV emission traces an excited cone of material above the disk and oriented along the jet axis, it may reveal the medium responsible for the torque that changed the alignment of the inner disk.

5. SUMMARY AND DISCUSSION

In this paper we have examined a near-infrared/visible colormap of the radio galaxy 3C 449, finding a twist in the isochromes. This twist is unexpected, as a planar disk should have isochromes aligned with the disk major axis and exhibiting reflective symmetry about the minor axis. The disk edge at a radius of ~ 600 pc has a major axis nearly (within 10°) coincident with the galactic isophotes (as seen at $1.6 \mu\text{m}$), suggesting that the outer disk has settled to the midplane of the galaxy. The isophotes at $1.6 \mu\text{m}$ reveal no evidence for a recent merger or a strongly triaxial bulge. Consequently, the twist in the isochromes is most likely due to the disk itself.

By integrating light through an absorptive thin disk model, we find that we can account for the twist in the isochromes with a warped geometry. The model predicts rotation along the minor axis of the outer disk that is consistent with the sign of mean velocities measured from spectroscopic observations by Noel-Storr et al. (2003). In relation to the warp model, the pattern of UV and $\text{H}\alpha + [\text{NII}]$ emission (Allen et al. 2002; Martel et al. 2000), brighter to the north of the nucleus, could be emission from above the disk, possibly in a wide cone oriented approximately along the jet axes. The UV emission in front of the disk and to the north of the nucleus would be easier to see than an opposing cone behind the disk and to the south. This suggests a possible explanation for the lack of UV emission south of the nucleus or associated with the disk on the western side.

A warp in a disk with a sharp outer edge is not necessarily unexpected. For example, NGC 7626's contains a dust lane that ends abruptly, suggesting that it has an outer edge similar to that seen in 3C 449. The disk in NGC 7626 is clearly warped (see images by Verdoes Kleijn et al. 1999), and could resemble that of 3C 449 if viewed at a lower inclination. The ionized inner disk of NGC 6251 is tilted with respect to its outer dusty disk that also exhibits a sharp outer edge (Ferrarese & Ford 1999).

Our model for the warped disk of 3C 449 predicts that it is nearly parallel to the jet axis at a radius of 600 pc, but twists and becomes nearly perpendicular to the jet at ~ 100 pc. We can find examples of other radio

galaxies which might exhibit similar warps. For example, the disk in NGC 7626 is nearly edge-on, and twists such that the disk is nearly perpendicular to the jets near the nucleus (see images from Verdoes Kleijn et al. 1999). 3C 465, NGC 5127 and NGC 7052 contain disks with sharp outer edges. For these disks, as is true for that of 3C 449, the pattern absorption is almost triangular, suggesting that there is a twist in the isochromes. The jets in NGC 7052 are 45° from its disk, and the inner disk could be nearly perpendicular to the jet (see images by Verdoes Kleijn et al. 1999). If the disks in 3C 465 and NGC 5127 are twisted, their inner disks would be nearly perpendicular to their jet axes (see images by de Koff et al. 2000 and by Verdoes Kleijn et al. 1999). 3C 236 contains an inner disk which is nearly perpendicular to its jets, whereas the outer disk is tilted about 25° degrees from its outer disk (de Koff et al. 2000). M84 (3C 272.1) has a similar inner and outer disk structure (Quillen & Bower 1999), and again the inner disk is more nearly perpendicular to the jet axis. NGC 6251 presents a counter example, as the inner ionized disk is not oriented along the jet axis (Ferrarese & Ford 1999). In the future, our procedure for modeling warped dusty disks could be used to study the disk geometries of these other objects.

The notion that our warp model for 3C 449 accounts for jet/disk orthogonality is somewhat mysterious. Since the rotation period is shorter at smaller radii, an initially misaligned disk should first settle into the galaxy midplane at its innermost edge. However, the disk of 3C 449 is settled into the symmetry plane at large radii but *not* in its inner regions. Such a morphology suggests that there is a force, aligned with or associated with the jets or active nucleus, that has pushed the disk preferentially at smaller radii.

We have considered the possibility that a torque associated with a nuclear binary black hole could affect the disk orientation. We have also noted that radiation pressure from a central source could cause the disk to precess, or that the radiative warp instability proposed by Pringle (1996) is playing a role. We have shown that the timescales associated with these scenarios are too long to account for the warp in the disk of 3C 449. The pressure in the X-ray emitting ISM, however, is likely to be large enough that this medium could perturb the disk. A static model with elongated isobars would only cause the disk to precess, not be pushed into the plane orthogonal to the jet axis. Such precession might be damped by processes internal to the disk (e.g., high viscosity, collisions, etc.), but the associated settling time would be of order the accretion timescale, which is again too long. Non-axisymmetric winds driven off the disk by evaporative, radiative, and MHD processes (like those discussed by Meyer & Meyer-Hofmeister 1994) are likely to play a role in the morphology of the disk, but not to a degree large enough to account for the warp. An interaction between the disk and the jet-excited ambient ISM (resulting in a drag force or inflow) could cause the disk to be pushed into the plane perpendicular to the jet, so long as there is sufficient turbulence and anisotropy in the X-ray emitting region. This suggests the intriguing possibility that studies of nuclear disk morphology can be used to probe past interactions between outflow-excited material and a comparatively cold gaseous disk. In the

case of 3C 449, the UV emission (visible only north of the nucleus) might help trace the intricacies of such an interaction.

A close look at images of disks in radio galaxies reveals not only warps but lopsidedness, sharp edges, and spiral features. Such observations are somewhat counterintuitive. Because of differential rotation, a lopsided disk should rapidly (on a few times the rotation period) become circular, a sharp edge should become smooth on a diffusion timescale (roughly the rotation period divided by the viscosity α parameter), and a non-self-gravitating disk should only exhibit transient spiral features. As such, the morphology of such disks suggests that they may have been recently perturbed, even truncated. Notably nonactive elliptical galaxies can contain disks which exhibit similar structures. It is possible that gaseous disks in elliptical galaxies are perturbed by present or past nuclear activity. Future high angular resolution studies could better probe this possible connection.

Such a relationship between nuclear disk morphology and the ambient ISM can be considered a specialized manifestation of “feedback” from an AGN. Accreting black holes release enormous amounts of energy to their surroundings in various forms (through heating, radiation pressure, and induced kinetic motions, as discussed

by Begelman 2004; Fabian et al. 2003). It is not unreasonable, then, to interpret structurally perturbed nuclear disks as consequences of current and past interactions between an AGN and its surrounding medium.

We gratefully acknowledge helpful discussions with David Merritt, Eric Blackman, Stephen Thorndike, Ivan Minchev, Kate Green, Russell Knox, and Amanda LaPage. We also thank George Privon for reduction of VLA data for 3C 449, and the anonymous referee whose valuable comments led to the improvement of this paper. This work was based on observations with the NASA/ESA *Hubble Space Telescope*, obtained in collaboration with the Space Telescope Science Institute (STScI), operated by AURA for NASA. Support for this work was provided by NASA/STScI through grant HST-GO-10173. G. R. T. and A. C. Q. acknowledge support in part by NSF awards AST-0406823, PHY-0242483, and NASA/STScI grant HST-GO-10173.09-A. This research has made extensive use of the NASA Astrophysics Data System (ADS) and the NASA/IPAC Extragalactic Database (NED), operated by the Jet Propulsion Laboratory, California Institute of Technology, under contract with the National Aeronautics and Space Administration.

REFERENCES

- Allen, M. G., Sparks, W. B., Koekemoer, A., Martel, A. R., O’Dea, C. P., Baum, S. A., Chiaberge, M., Macchetto, F. D., & Miley, George K. 2002, *ApJS*, 139, 411
- Armitage, P. J., Natarajan, P. 1999, *ApJ*, 525, 909
- Bardeen, J. M., & Petterson, J. A. 1975, *ApJ*, 193, L65
- Begelman, M. C. 2004, *Coevolution of Black Holes and Galaxies*, from the Carnegie Observatories Centennial Symposia. Published by Cambridge University Press, as part of the Carnegie Observatories Astrophysics Series. Edited by L. C. Ho, p. 375.
- Bettoni, D., Falomo, R., Fasano, G., & Govoni, F. 2003, *A&A*, 399, 869
- Capetti, A., Celotti, A., Chiaberge, M., de Ruiter, H. R., Fanti, R., Morganti, R., & Parma, P. 2002, *A&A*, 383, 104
- Caproni, A., & Abraham, Z. 2004, *ApJ*, 602, 625
- Chiaberge, M., Capetti, A., & Celotti, A. 1999, *A&A*, 349, 77
- Chiaberge, M., Gilli, R., Capetti, A., & Macchetto, F. D. 2003, *ApJ*, 597, 166
- Cornwell, T., & Perley, R., 1984, in Bridle A. H., Eilek J. A., eds, *Physics of Energy Transport in Radio Galaxies*, NRAO Workshop No. 9. NRAO, Green Bank, West Virginia, p. 39
- de Koff, S., Baum, S. A., Sparks, W. B., Biretta, J., Golombek, D., Macchetto, F., McCarthy, P., & Miley, G. K. 1996, *ApJS*, 107, 621
- de Koff, S., Best, P., Baum, S. A., Sparks, W., Rottgering, H., Miley, G., Golombek, D., Macchetto, F., & Martel, A. 2000, *ApJS*, 129, 33
- Donato, D., Sambruna, R. M., & Gliozzi, M. 2004, *ApJ*, 617, 915
- Fabian, A. C., Sanders, J. S., Allen, S. W., Crawford, C. S., Iwasawa, K., Johnstone, R. M., Schmidt, R. W., & Taylor, G. B. 2003, *MNRAS*, 344, 43
- Fanaroff, B. L. & Riley, J. M. 1974, *MNRAS*, 167, 31p
- Ferrarese, L., Ford, H. C., & Jaffe, W. 1996, *ApJ*, 470, 444
- Ferrarese, L., & Ford, H. C. 1999, *ApJ*, 515, 583
- Ferrarese, L., & Merritt, D. 2000, *ApJ*, 539, L9
- Feretti, L., Perley, R., Giovannini, G. & Andernach, H. 1999, *A&A*, 341, 29
- Gebhardt, K. et al. 2000, *ApJ*, 543, L5
- Gebhardt, K. et al. 2003, *ApJ*, 583, 92
- Goudfrooij, P., & de Jong, T. 1995, *A&A*, 298, 784
- Gower, A., & Hutchings, J. B. 1982, *ApJ*, 258, L63
- Hardcastle, M. J., Worrall, D. M., & Birkinshaw, M. 1998, *MNRAS*, 296, 1098
- Jaffe, W., Ford, H., Ferrarese, L., van den Bosch, F., & O’Connell, R. W. 1996, *ApJ*, 460, 214
- Kinney, A.L., Schmidt, H.R., Clarke, C. J., Pringle, J.E., Ulvestad, J.S., & Antonucci, R.R.J. 2000, *ApJ*, 537, 152
- Kotanyi, C., & Ekers, R. 1979, *A&A*, 73, L1
- Kumar, S., & Pringle, J. E. 1985, *MNRAS*, 213, 435
- Lauer, T. et al. 2005, *AJ*, 129, 2138
- Lense, J., & Thirring, H. 1918, *Phys. Z.*, 19, 156
- Liu, F. K. 2004, *MNRAS*, 347, 1357
- Lubow, S. H., Ogilvie, G. I., & Pringle, J. E. 2002, *MNRAS*, 337, 706
- Madrid, J.P., Chiaberge, M., Floyd, D., Sparks, W.F., Macchetto, D., Miley, G.K., Axon, D., Capetti, A., O’Dea, C., Baum, S., Perlman, E. S., & Quillen, A. C. 2005, in preparation
- Mathis, J. S. 1990, *ARA&A*, 28, 37
- Macchetto, F., McCarthy, P., & Miley, G. K. 1996, *ApJS*, 107, 621
- Maloney, P. R., Begelman, M. C., & Pringle, J. E. 1996, *ApJ*, 472, 582
- Martel, A., Turner, N., Sparks, W., Baum, S. 2000, *ApJS*, 130, 267
- McCarthy, P. et al. 1997, *ApJS*, 112, 415
- Merritt, D., & Ekers, R. D. 2002, *Science*, 297, 1310
- Meyer, F., & Meyer-Hofmeister, E. 1994, *A&A*, 288, 175
- Milosavljevic, M., & Merritt, D. 2003, *ApJ*, 596, 860
- Möllenhoff, C., Hummel, E., & Bender, R. 1992, *A&A*, 255, 35
- Natarajan, P., & Pringle J. E. 1998, *ApJ*, 506, L97
- Noel-Storr, J., Baum, S. A., Verdoes Kleijn, G., van der Marel, R. P., O’Dea, C. P., de Zeeuw, P. T., & Carollo, C. M. 2003, *ApJS*, 148, 419
- Noel-Storr, J., Baum, S. A., O’Dea, C. P. et al. 2005, in preparation
- O’Dea, C. P., Koekemoer, A.M., Baum, S.A., Sparks, W.B., Martel, A.R., Allen, M.G., Macchetto, F.D., & Miley, G.K. 2001, *AJ*, 121, 1915
- Peng, C. Y., Ho, L. C., Impey, C. D., & Rix, H. 2002, *AJ*, 124, 266
- Pringle, J. E. 1996, *MNRAS*, 281, 357
- Prugniel, P., & Simien, F. 1997, *A&A*, 321, 111
- Quillen, A. C., & Bower, G. 1997, (astro-ph/9709107)
- Quillen, A. C., & Bower, G. 1999, *ApJ*, 522, 718
- Quillen, A. C., Alonso-Herrero, A., Rieke, M. J., McDonald, C., Falcke, H., & Rieke, G. H. 1999, *ApJ*, 525, 685
- Quillen, A. C. 2001, *ApJ*, 563, 313
- Rees, M. J. 1978, *Nature*, 275, 516
- Rees, M. J., Begelman, M. C., Blandford, R. D., & Phinney, E. S. 1982, *Nature*, 295, 17

- Rees, M. J. 1984, *ARA&A*, 22, 271
- Sansom, A. E. et al. 1987, *MNRAS*, 229, 15
- Scheuer, P. A. G., & Feiler, R. 1996, *MNRAS*, 282, 291
- Schmitt, H. R., Pringle, J. E., Clarke, C. J., & Kinney, A. L. 2002, *ApJ*, 575, 150
- Solrzano-Iarrea, C., Tadhunter, C. N., & Bland-Hawthorn, J. 2002, *MNRAS*, 331, 673
- Sparks, W. B., Baum, S. A., Biretta, J., Macchetto, F. D., & Martel, A. R. 2000, *ApJ*, 542, 667
- Steiman-Cameron, T. Y., & Durisen, R. H. 1988, *ApJ*, 325, 26
- Tran, H. D., Tsvetanov, Z., Ford, H. C., & Davies, J. 2001, *AJ*, 121, 2928
- Tremaine, S. et al. 2002, *ApJ*, 574, 740
- van Dokkum, P. D., & Franx, M. 1995, *AJ*, 110, 2027
- Verdoes Kleijn, G. A., Baum, S. A., de Zeeuw, P. T., & O'Dea, C. P. 1999, *AJ*, 118, 2592
- Verdoes Kleijn, G. A., & de Zeeuw, P. T. 2005, *A&A*, 435, 43